SLEEPJ, 2021, 1–13

https://doi.org/10.1093/sleep/zsab170
Advance Access Publication Date: 8 July 2021
Original Article

ORIGINAL ARTICLE

Frequency of flow limitation using airflow shape

Dwayne L. Mann[1,2,3,*], Thomas Georgeson[1,4,§], Shane A. Landry[3,5,§], Bradley A. Edwards[3,5], Ali Azarbarzin[6], Daniel Vena[6], Lauren B. Hess[6], Andrew Wellman[6], Susan Redline[6], Scott A. Sands[6,#] and Philip I. Terrill[1,#]

[1]School of Information Technology and Electrical Engineering, University of Queensland, Brisbane, Australia, [2]Institute for Social Science Research, University of Queensland, Brisbane, Australia, [3]Department of Physiology, School of Biomedical Sciences and Biomedical Discovery Institute, Monash University, Melbourne, Australia, [4]Faculty of Medicine, University of Queensland, Brisbane, Australia, [5]School of Psychological Sciences and Turner Institute for Brain and Mental Health, Monash University, Melbourne, Australia and [6]Division of Sleep and Circadian Disorders, Department of Medicine, Brigham & Women's Hospital & Harvard Medical School, Boston, MA, USA

[§]These authors contributed equally to this work in a different capacity.
[#]These authors contributed equally.

*Corresponding author. Dwayne L. Mann, Institute for Social Science Research, The University of Queensland, Brisbane, Australia. Email: d.mann@uq.edu.au.

Abstract

Study Objectives: The presence of flow limitation during sleep is associated with adverse health consequences independent of obstructive sleep apnea (OSA) severity (apnea-hypopnea index, AHI), but remains extremely challenging to quantify. Here we present a unique library and an accompanying automated method that we apply to investigate flow limitation during sleep.

Methods: A library of 117,871 breaths (N = 40 participants) were visually classified (*certain* flow limitation, *possible* flow limitation, *normal*) using airflow shape and physiological signals (ventilatory drive per intra-esophageal diaphragm EMG). An ordinal regression model was developed to quantify flow limitation certainty using flow-shape features (e.g. flattening, scooping); breath-by-breath agreement (Cohen's $\hat{\kappa}$); and overnight flow limitation frequency (R^2, $\%_{breaths}$ in certain or possible categories during sleep) were compared against visual scoring. Subsequent application examined flow limitation frequency during arousals and stable breathing, and associations with ventilatory drive.

Results: The model (23 features) assessed flow limitation with good agreement (breath-by-breath $\hat{\kappa}$ = 0.572, $p < 0.001$) and minimal error (overnight flow limitation frequency R^2 = 0.86, error = 7.2%). Flow limitation frequency was largely independent of AHI (R^2 = 0.16) and varied widely within individuals with OSA (74[32–95]$\%_{breaths}$, mean[range], AHI > 15/h, N = 22). Flow limitation was unexpectedly frequent but variable during arousals (40[5–85]$\%_{breaths}$) and stable breathing (58[12–91]$\%_{breaths}$), and was associated with elevated ventilatory drive (R^2 = 0.26–0.29; R^2 < 0.01 AHI *v.* drive).

Conclusions: Our method enables quantification of flow limitation frequency, a key aspect of obstructive sleep-disordered breathing that is independent of the AHI and often unavailable. Flow limitation frequency varies widely between individuals, is prevalent during arousals and stable breathing, and reveals elevated ventilatory drive.

Clinical trial registration: The current observational physiology study does not qualify as a clinical trial.

Statement of Significance

Flow limitation during sleep is the defining feature of obstructive sleep-disordered breathing, yet—due to lack of expert consensus and automated methods—is routinely absent from clinical reports. Here we developed a library of physiologically informed, visually classified breaths from which we developed an automated flow-shape model to (1) quantify the certainty of flow limitation for any breath and (2) measure overnight flow limitation frequency. We found that frequent flow limitation can occur despite low apnea-hypopnea index (AHI); pronounced flow limitation also was observed during arousals and stable breathing. Flow limitation but not AHI detected elevated respiratory drive/effort. Our approach provides a much-needed means to objectively quantify the frequency of obstructive sleep-disordered breathing that is otherwise unreported.

Key words: airflow obstruction; inspiratory flow limitation; upper airway resistance syndrome; diaphragm EMG; polysomnography; phenotype; classification; automated

Submitted: 6 March, 2021; **Revised:** 27 June, 2021

Introduction

Pharyngeal inspiratory flow limitation (or airflow obstruction), characterized by a failure of airflow to reach the intended levels based on neural drive, is the defining feature of obstructive sleep-disordered breathing [1, 2]. Episodic flow limitation that leads to reduced airflow manifests as obstructive apneas and hypopneas and is routinely quantified using the apnea-hypopnea index (AHI). Yet the AHI does not capture the form of obstructive sleep-disordered breathing that is typically accompanied by sustained flow limitation and increased ventilatory effort or drive to breathe rather than episodic hypoventilation (apneas/hypopneas) [3, 4]. Research has recently highlighted that the AHI is not strongly associated with sleep-disordered breathing symptoms or outcomes, and accumulating evidence suggests that the frequency of flow limitation may play a key role [5–13]. However, there is no widely available clinically applicable way to objectively and automatically measure the frequency of flow limitation during sleep.

There is active interest in the development of noninvasive methods to automatically detect inspiratory flow limitation, particularly using the flow "shape" of individual breaths [1, 14–23]. While several approaches have emerged [14–23], major limitations include (1) the use of expert training data that is not guided by physiological signals that inform whether ventilation (*flow*) meets intended levels (*drive*) and (2) the lack of algorithm accessibility. On the other hand, our prior method using direct physiological measurement of *flow:drive* [2] did not leverage human expertise to guide classification. At present, there is no available method to classify flow limitation that is based on a combination of visual interpretation and gold standard invasive physiological information. Such a method is needed to automatically and objectively measure the *frequency* of flow limitation during sleep, and thereby supplant the current use of subjective, time-consuming clinical scoring [1, 24, 25].

Accordingly, the current study sought to provide an automated method to detect flow limitation during sleep. To achieve this goal, we developed a unique library of 100,000+ breaths visually scored as certain flow limitation, possible flow limitation, or normal based on the observed airflow shape, gold standard physiological signals (calibrated airflow and ventilatory drive by intra-esophageal diaphragm EMG), and other contemporaneous polysomnographic information. Subsequently, we developed an objective flow-shape-based multivariable ordinal logistic regression model to calculate the *certainty* of flow limitation of individual breaths, which can be readily translated for clinical use. First, the method was validated by assessing scoring agreement at a breath level (kappa coefficient) and the extent to which the method captures flow limitation frequency on a patient-level (coefficient of determination and mean absolute error). We also quantified the importance of including visual scoring and examined the threshold levels of physiological obstruction (*flow:drive*) that was visually classified as flow limited. Second, we determined the extent to which the method provides unique information beyond the AHI. Third, in patients with obstructive sleep apnea (OSA), we applied the method to examine the prevalence of flow limitation during arousals and stable breathing periods when respiratory mechanics are often thought to be minimally compromised. We also assessed whether the measure is capable of detecting elevated ventilatory drive independent of AHI.

Methods

Subjects

Participants with suspected or diagnosed sleep apnea were enrolled in a single night physiology study examining ventilation and ventilatory drive (intra-esophageal diaphragm EMG). Exclusion criteria included severe comorbidities (heart failure [i.e. ejection fraction < 45%], lung diseases [forced expiratory ratio < 65% or resting pulse oxygen saturation < 94% at rest], known kidney disease [eGFR < 50 mL/min/1.73m^2], neuromuscular diseases, and neurodegenerative diseases), central sleep apnea (greater than 50% of events), pregnancy, and medications known to stimulate or depress respiration (including acetazolamide, theophylline, opioids, benzodiazepines, and barbiturates). A total of 43 participants were enrolled: $N = 1$ refused intraesophageal catheter after the consent, $N = 1$ had a strong gag reflex and did not tolerate catheter placement, and $N = 1$ patient was not studied without continuous positive airway pressure (CPAP) connected, leaving 40 participants for analysis. The study was approved by the Partners Human Research Committee. Patients signed written informed consent before participation.

Equipment

In addition to routine polysomnographic signals (electroencephalography, electrocardiography, thoracoabdominal movements, and oximetry), airflow was measured with a pneumotach (Hans Rudolf, Shawnee, KS; Validyne Engineering, Northbridge, CA) via a sealed oronasal mask (AirFit small, Resmed Inc., San Diego, CA). The ventilatory drive was measured via multichannel intra-esophageal diaphragm EMG (Maquet Getinge Group, Wayne, NJ), placed such that the central electrodes provided the strongest signals; EMG deflections (rms, peak minus pre-inspiratory baseline) were calibrated to units of L/min using wakefulness data [2]. In 17 participants, nasal pressure was measured via nasal cannula (Hudson RCI Over-the-ear, Teleflex, Morrisville, NC; referenced to mask pressure to reveal the transnare pressure difference seen clinically). In 40 participants, esophageal pressure measurements (Millar, Inc., Houston, TX) were also made; the pressure sensor was first advanced into the stomach, then withdrawn back to the esophagus as determined by negative inspiratory deflections, and further withdrawn another ~5 cm).

Visual scoring

A single experienced sleep technician (TG) scored all available breaths according to the following protocol.

Protocol for visual scoring. We developed a visual scoring protocol to classify individual breaths as exhibiting certain flow limitation (certain FL); possible flow limitation (possible FL); or normal flow. The scoring protocol used primary criteria based on (1) expert human assessment of flow shape combined with (2) an objective measure describing the ratio of ventilation to ventilatory drive (termed *flow:drive* [2]) and (3) where necessary, secondary criteria based on associative contextual information (e.g. EEG, SpO_2, etc.). This approach was designed to overcome measurement noise in

any individual physiological signal. Table 1 summarises the scoring guidelines. See Supplement for full details.

Visual scoring platform. We developed custom software (written in MATLAB) to facilitate visual breath-by-breath scoring according to the protocol described in the previous paragraph (Figure S1) of all breaths, irrespective of sleep staging and clinical scoring. Accordingly, flow limitation was scored in "Wake" when present (e.g. during 30-second Wake epochs that included transitional sleep).

In addition to the three defined breath types (certain FL, possible FL, or normal), the scorer could also classify a breath as being of poor signal quality (e.g. movement, noise, etc.). Such breaths were excluded from further analysis in this study.

Inter-scorer agreement

A second expert (SL) independently assessed and scored 100 consecutive breaths from each third of each study using the same protocol and custom scoring software described in the previous section. This process was intended to test the independent application of the developed protocol, and assess if scoring was consistent between scorers, both within and across patients.

Novel objective flow-shape model of flow limitation

Following the visual classification of all breaths, we subsequently developed a simplified regression model using airflow shape features to predict these categories that could be readily shared with future investigators.

Flow shape measures and feature transformations. Model development was based on 85 candidate pneumotachograph-derived flow shape measures (features) described previously [2]. In brief, flow signals were downsampled to 25 Hz (AASM minimum recommended) to provide generalizability. For each breath, multiple features were quantified that captured (1) flattening; (2) scooping, or the deviation away from normal rounded contour; (3) asymmetry; (4) timing and volume ratio measures; and (5) futtering and spectral properties. To capture potential non-linearity between flow-shape features and flow limitation, transformed versions (squared and square-root) of the flow-shape features were made. The transformed versions together with the untransformed version of all flow-shape features were available for model selection (called "feature terms").

Model development and feature selection

Ordinal logistic regression was used to predict the three visually scored flow limitation categories (certain flow limitation, possible flow limitation, normal; dependent variable) using the feature terms (continuous independent variables). For the selection of feature terms, a stepwise algorithm (sequential forward floating search [26, 27]) was used to efficiently add feature terms to incrementally improve model performance (minimum increment in Cohen's Kappa of $\kappa = 0.005$). Logistic regression cutoffs were determined by maximizing sensitivity plus specificity [28].

Cross-validation

A leave-one-participant-out cross-validation procedure (entire process including feature selection) was performed to provide additional conservative performance results (breath-level agreement, and patient-level associations). Specifically, all model predictions for a given participant were determined using a modified version of the model developed with the participant's data held out.

Table 1. Visual assessment of flow limitation

		Physiological *flow:drive* categorization			
		Normal (>80%)	Mild (50%–80%)	Moderate (30%–50%)	Severe (<30%)
Flow shape categorization	**Normal** Sinusoidal or representative of wakefulness breath shapes	Normal	Normal* or Possible FL†	Possible FL	Certain FL
	Mild A slight element of flattening, scooping, shaving, or fluttering	Normal* or Possible FL†	Possible FL	Possible* or Certain† FL	Certain FL
	Moderate <80% of the intended breath volume is achieved	Possible FL	Possible* or Certain† FL	Certain FL	Certain FL
	Severe <50% of the intended breath volume is achieved	Certain FL	Certain FL	Certain FL	Certain FL

*Without relevant associative criteria, described below.

†With relevant associative criteria.

FL, flow limitation. To support visual classification based on the raw airflow traces, scorers had access to calculated values of *flow:drive* ratio per diaphragm EMG (50% indicates ventilation was half the intended value based on the neural ventilatory drive) and, in addition, values of ventilation (L/min), processed diaphragm EMG traces (μV), estimated *flow:drive* per published flow shape model [2], and the option to display esophageal pressure traces (cmH_2O). Secondary criteria, that is, associative information was used as categorical modifiers in borderline cases (e.g. snoring, arousal desaturation, flow shape, neighboring signals, see Supplement for details). Associative criteria included: prolonged inspiratory time, relative to total breath time; strong snoring signal overlaying pressure (snore amplitude >20% of the flow amplitude); EEG suggestive of respiratory effort-related arousal (e.g. sub-clinical arousal); SpO_2 desaturation (>2%) suggestive of sub-eupneic ventilation; unusually shaped breaths (i.e. not characteristic of normal flow shape); and expiratory obstruction.

Analysis of nasal pressure

The above model was also applied to estimate flow limitation using linearized (two-thirds power transform) nasal pressure derived flow shapes (subset of $N = 17$ participants) for additional validation.

Frequency of flow limitation breaths

All breaths during sleep (including all sleep stages, scored events, and scored arousals) were considered for the measurement of "flow-limitation frequency." Two measures were considered: (1) frequency of "certain" flow limitation and (2) frequency of "possible + certain" flow limitation, expressed as a percentage of the total number of breaths analyzed. Breaths during obstructive apneas (where flow is absent and shape information is unavailable) were automatically considered as certain flow-limited for this analysis. These measures were calculated separately using pneumotach and nasal pressure data.

In additional analyses, we calculated the frequency of flow limitation during (1) arousals and (2) during stable breathing (periods of sleep > 3 min duration without scored respiratory events or arousals).

Arousal breaths were scored based on standard AASM guidelines, that is, >3 s duration abrupt shift in EEG frequency (beta, alpha, theta, but not spindles) with two exceptions optimized for physiological assessment: arousals had no maximal duration, and arousals that were observed within 10 s of prior arousal were not removed (In this way, periods of sleep without arousal markings could be considered free from arousals.). For analysis of arousals, however, we emphasize that breaths within epochs of wake were removed (i.e. for long arousals in sleep that ultimately led to wake, only the breaths within the sleep epochs were included.

Statistical analysis

All statistical analyses were performed using MATLAB Statistics Toolbox. $p < 0.05$ was considered statistically significant. Average values are presented as mean ± SD, or mean[range] as appropriate.

Main analysis for individual breath classification. Cohen's Kappa was used to quantify the overall breath-by-breath agreement between flow shape model categories of flow limitation (3-class prediction) and visual-scored flow limitation categories (3-class standard). A value of 0 represents chance agreement and 1 represents perfect classification; we sought a value exceeding 0.4 (moderate agreement).

We also report accuracy for two-group discrimination (certain flow limitation *v.* normal), that is, the sum of correct predictions over total predictions with the possible flow limitation category omitted.

Main analysis for frequency of flow limitation assessment. Linear regression R^2 values were used to compare flow-shape estimates (independent variable in assessment) versus visual scoring measures (dependent variable in assessment) of flow limitation frequency during sleep; a value ≥ 0.5 was considered a strong association. Co-primary measures ("certain," "possible + certain") were based on pneumotach flow shape ($p < 0.025$ used as the significance level for multiplicity). An absolute error was quantified by mean absolute value, with the goal of a value below 15%.

To confirm clinical translatability, the above analyses were repeated using the nasal pressure signal. Specifically, flow shapes derived from nasal pressure were applied to the existing model to classify flow limitation (for comparison with visual scoring).

Table 2. Participant characteristics

Characteristics	Comparison to gold standards ($N = 40$)	Nasal pressure *v.* pneumotach ($N = 17$)
Demographics		
Age (years)	57 ± 9	59 ± 9
Sex (M:F)	24:16	11:6
Race (Black:White:Asian:Other)	12:27:0:1	3:14:0:0
Body mass index (kg/m^2)	32.5 ± 6.6	31.8 ± 7.5
Neck circumference (cm)	41.4 ± 4.9	41 ± 5.2
Currently treated (CPAP:oral appliance:untreated)	15:2:23	2:1:14
Polysomnography		
OSA severity (normal:moderate-to-severe)	18:22	12:5
Apnea-hypopnea index, total (events/h)	29.2 ± 26.4	15.4 ± 15.7
Apnea-hypopnea index, non-REM (events/h)	28.7 ± 27.1	14.5 ± 16.1
Central events, non-REM (% respiratory events)	0.2 ± 0.8	0.5 ± 1.2
Hypopneas, non-REM (% respiratory events)	66.0 ± 29.9	80.3 ± 21.7
Arousal index, non-REM (events/h)	49.5 ± 23.9	42.7 ± 18.4
Total sleep time (min)	241 ± 93	249 ± 80
Sleep time, spontaneous breathing* (min)	164 ± 95	209 ± 83
Non-REM 1 (% total sleep time)	37 ± 21	37 ± 23
Non-REM 2 (% total sleep time)	48 ± 17	46 ± 18
Non-REM 3 (% total sleep time)	6 ± 7	8 ± 10
REM (% total sleep time)	9 ± 8	9 ± 9

*Reflects the sleep time available for analysis without physiological tests.

Values are mean ± S.D. OSA severity classes defined as normal or mild OSA (apnea-hypopnea index, AHI < 15); moderate-to-severe OSA (AHI ≥ 15 events/h). CPAP, continuous positive airway pressure; OSA, obstructive sleep apnea; REM, rapid-eye-movement sleep; AHI, apnea-hypopnea index. Note the lower AHI in the nasal pressure subset was not by design.

Results

Participant characteristics are described in Table 2.

Interscorer agreement

117,871 breaths were classified from 40 patients during wakefulness and sleep. The second expert human assessor independently scored 12,005 breaths (~10% of all processed breaths). Agreement between the two expert assessors for the 40 patients was excellent ($\hat{\kappa}$ = 0.74 pooled breaths, Table S1; patient average $\hat{\kappa}$ = 0.66 ± 0.15; mean ± SD).

Relationship between physiological severity and visual classification

Physiological measurement of obstruction severity. The relationship between visual classification and gold-standard physiological measurement of *flow:drive* by diaphragm EMG is shown in Figure 1A. Average *flow:drive* fell progressively with increasing categorical classification of certainty of flow limitation (mean ± SD: 106 ± 22%, 78 ± 21%, and 46 ± 19% for normal, possible flow limitation, and certain flow limitation categories, respectively). Threshold physiological obstruction levels for each category of flow limitation are provided in Figure 1.

Novel objective flow-shape model of flow limitation

A 3-class ordinal logistic regression model combined 23 airflow shape measures to classify breaths based on flow limitation certainty (normal, possible, or certain flow limitation; Table S2 for full regression model). The model illustrated moderate agreement between flow shapes and visual scoring (prior to cross-validation: $\hat{\kappa}$ = 0.572, 2-class accuracy = 94.3%, Table S3). The continuous model output (probability of flow limitation, certain + possible) for all breaths in each class (normal, possible, or certain are shown in Figure 1B. Example breaths in each class are shown with accompanying objective probability scores (Figure 2).

Cross-validation. After cross-validation, the predictive classification performance of the model applied to pneumotach flow data remained moderate ($\hat{\kappa}$ = 0.529, 2-class accuracy = 92.4%, Table S4). Application of the model to nasal pressure data

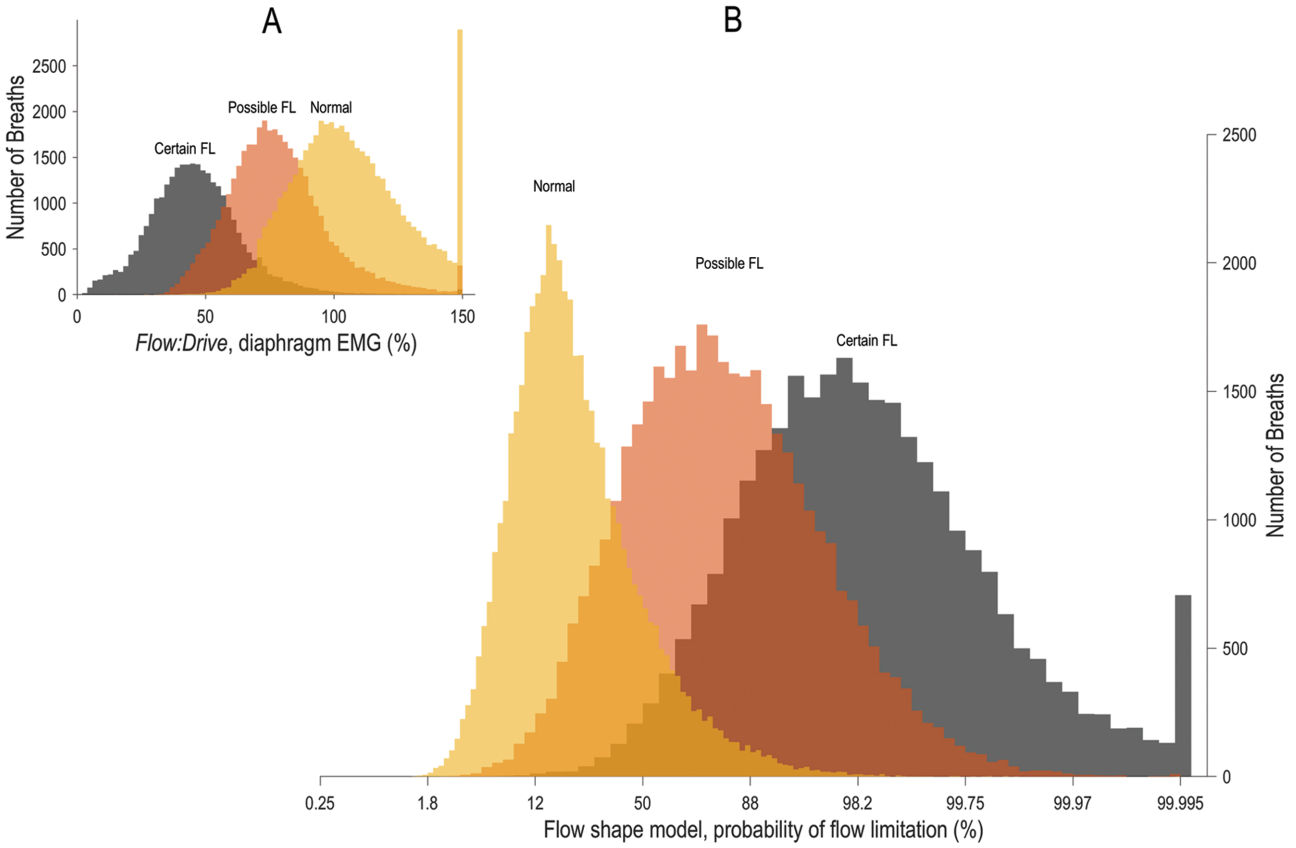

Figure 1. Histograms illustrating differences in breaths from each visually scored flow-limitation category (gray, certain flow limitation; "Certain FL," N = 29,080; orange, possible flow limitation "Possible FL," N = 39,053; yellow, "Normal," N = 49,738). Differences between categories are shown for (A) physiologically measured airflow obstruction severity (*flow:drive* per diaphragm EMG) where lower values indicate more severe obstruction and (B) novel flow shape model developed in the current study to estimate the probability of flow limitation (23-feature ordinal logistic regression model). Note clear group separation between certain flow limitations and normal categories (gray *v.* yellow). Optimal thresholds to separate certain from possible, and possible from normal in (A) were 58% and 86%, respectively (2-class threshold separating certain from normal: 70%), and in (B) were 50% and 95.7% (2-class threshold: 75%). Greater *x*-axis distance in (B) represents a higher log-odds score based on the linear combination of features in the regression model; 12%, 50%, and 88% probability is equivalent to log-odds of flow limitation of –2, 0, and +2, respectively.

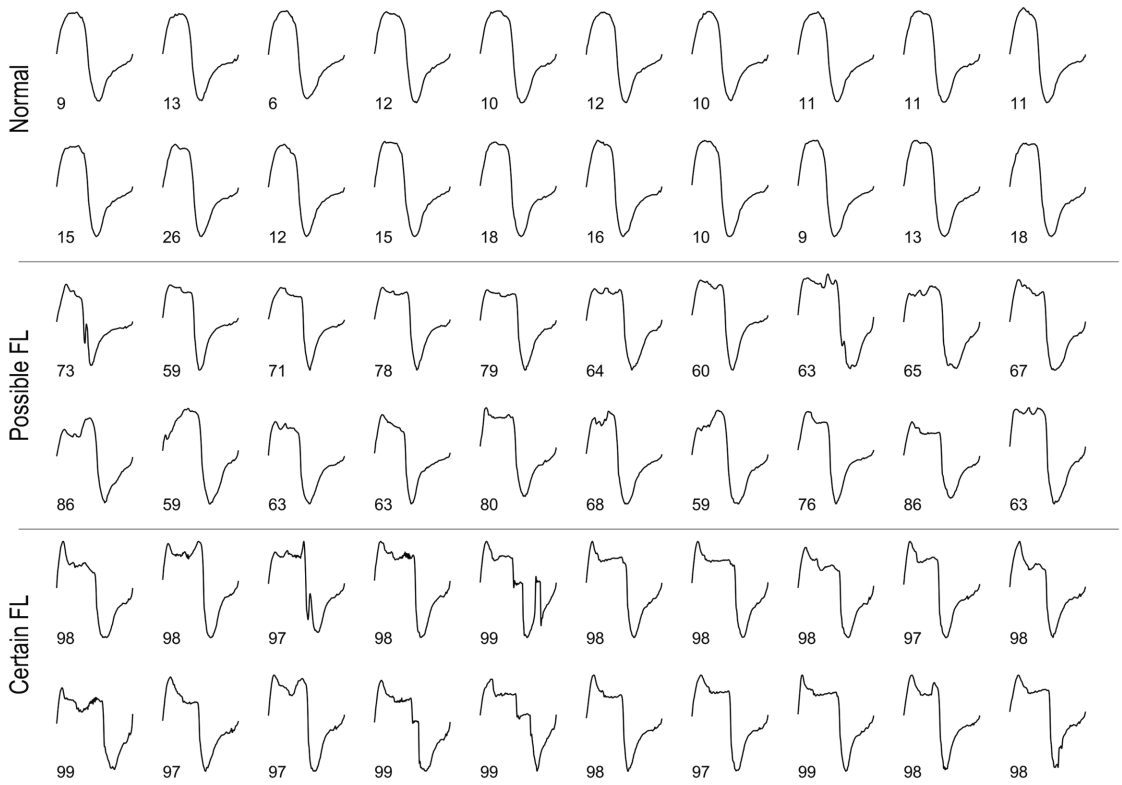

Figure 2. Example pneumotach flow traces for breaths visually scored as normal, possible flow limitation "Possible FL," and certain flow limitation "Certain FL" for an individual patient. Figures for other patients are provided in the Online Supplement and are intended to provide a resource upon which readers can use to calibrate visual scoring of flow limitation across centers. Numbers accompanying each breath illustrate the flow shape model-estimated percent probability of flow limitation (ordinal logistic regression model). The figure illustrates the continuum of certainty in flow limitation from Normal to Possible to Certain flow limitation categories; breaths at the top are rounded, while those lower on the page exhibited greater flattening and scooping illustrating that the intended airflow is lower than the achieved level. Note also the heterogeneity in shapes for breaths within this single subject.

yielded moderate cross-validated performance (ƙ = 0.442, 2-class accuracy = 88.2%, respectively, Table S5).

Benefit of informed visual scoring over physiological measurement

To examine whether visual scoring provided an incrementally stronger association with airflow shapes than that afforded by physiologically measured obstruction severity (using diaphragm EMG) alone, we used ordinal regression to associate flow shapes with *flow:drive*-based categories (cutoffs set to maintain proportions per visual scoring). Agreement between *flow:drive* and flow shapes was considerably weaker (ƙ = 0.379, 2-class accuracy = 86.3%, Table S6) than for the model linking informed visual scoring to flow shapes (compare with ƙ = 0.572 above); note the difference in ƙ is taken to reflect the visual scoring contribution to the agreement.

Patient-level validation: frequency of flow limitation

For each participant, we examined the frequency of flow limitation during sleep. Model-estimated flow limitation frequency (certain + possible) during sleep compared favorably with measures obtained from visual scoring (Figure 3A, $R^2 = 0.86$, $p < 0.025$, error = 7.2%). Results were also strong when defining the frequency of flow limitation using certain only breaths (Figure 3B, $p < 0.025$). Results after cross-validation remained strong (see Online Supplement, Figure S3, $p < 0.025$ for both).

Results were not meaningfully weaker with the use of nasal pressure in place of pneumotach ventilation to calculate flow shapes (Figure S4). Similarly, nasal pressure results remained strong after cross-validation (Figure S5).

Relationship between flow limitation and AHI

As expected, more severe flow limitation (objective *flow shape* scoring) was associated with a greater frequency of respiratory events (AHI, Figure 4A). Note however the broad range of severities of flow limitation for any given AHI. On average, in patients with moderate to severe OSA (AHI > 15 events/h), patients exhibited flow limitation (certain + possible) during sleep for 74[32–95]% (mean[range]) of the night, with 39[5–79]% of sleep certainly flow limited (based on objective *flow shape* scoring, Figure 4B). Proportions of flow-limited breaths were lowest during wakefulness (Figure 4C) and highest during obstructive hypopneas (Figure 4D), as expected. The prevalence of flow limitation breaths was similar between visual and objective scoring (Figure 4B–D).

Assessment of flow limitation in arousals and stable breathing

Here we seek to provide novel physiological insight into the prevalence of flow limitation during arousals and stable breathing in OSA and examine relationships with OSA severity.

Arousals are known to restore airflow following respiratory events in patients with sleep apnea, but in many cases,

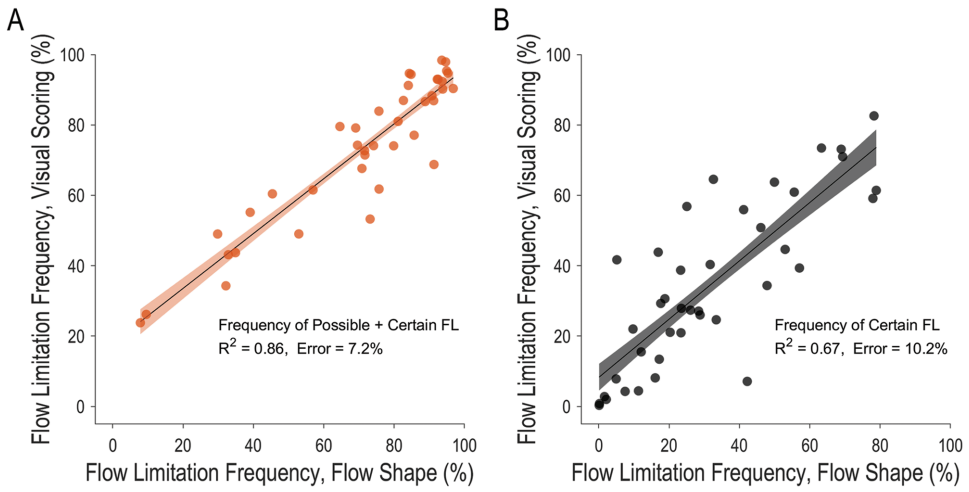

Figure 3. Frequency of flow limitation during sleep. Comparison between visual scoring and flow shape model measurements. The figure shows analysis based on pneumotach flow data prior to cross-validation. (A) The correlation between proportions of sleep breaths categorized as possible + certain flow limitation by the flow shape model versus visual scoring (after cross-validation $R^2 = 0.76$). (B) Analysis repeated for certain flow limitation (after cross-validation $R^2 = 0.53$). FL, flow limitation; R^2, coefficient of determination; Error, mean absolute error.

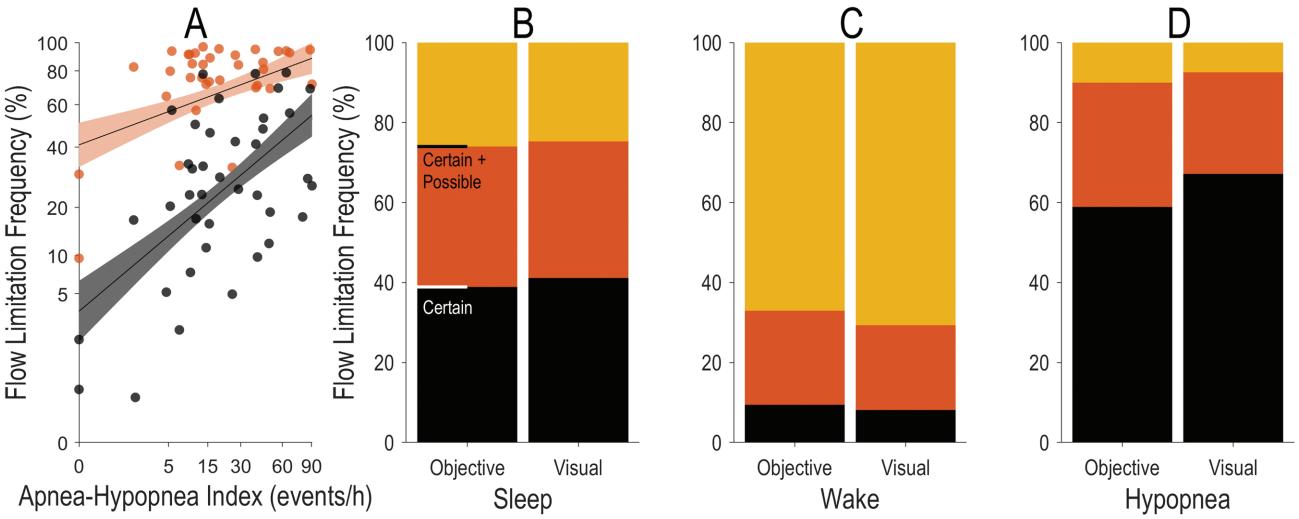

Figure 4. (A) Relationship between flow limitation frequency during sleep (flow shape model, "objective") and the apnea-hypopnea index (AHI; black dots show certain flow limitation, $R^2 = 0.33$, $p < 0.001$; orange dots show certain + possible flow limitation, $R^2 = 0.16$, $p < 0.05$). Data from all participants are shown ($N = 40$). Flow limitation frequency is shown for both flow shape model ("objective") and visual scoring ("visual") measurements during: (B) Sleep, (C) Wake, and (D) Obstructive Hypopneas. Stacked bars in panels B–D show group mean results from participants with obstructive sleep apnea (OSA, AHI > 15 events/h). As expected, we find that the majority of breaths during sleep in patients with OSA are flow limited. Also confirming methodological validity: most breaths during wake were scored as not flow limited (panel C, see Online Supplement Figure S6 for results in non-OSA) and most breaths within obstructive hypopneas were scored as flow limited (panel D).

the airway can remain flow limited. Figure 5A shows examples without and with flow limitation during hypopnea-related arousals. On average, in patients with OSA, flow-limitation was observed surprisingly frequently during arousals (certain + possible: 40[5–85]%, certain: 14[1–45]%), Figure 5B; greater levels of flow limitation during arousals were seen in those with more severe OSA (per higher AHI, Figure 5C). However, there was substantial heterogeneity in whether arousals were flow limited or not between participants (Figure 5D, contrast top row *v.* bottom row).

Likewise, stable breathing in patients with OSA is often thought to reflect a time with improved airway mechanics, however severe flow limitation is often observed [3, 29]. Figure 6A shows examples without and with flow limitation during stable breathing in OSA patients. Flow-limitation was observed surprisingly frequently during stable breathing (certain + possible: 58[12–91]%, certain: 28[2–64]%, Figure 6B); greater levels of flow limitation during stable breathing were typically observed with more severe OSA (Figure 6C). However, there was substantial heterogeneity in whether stable breathing was flow limited or not between participants (Figure 6D, contrast top row *v.* bottom row).

Flow limitation breath frequency as a measure of elevated respiratory effort

We demonstrated that greater flow limitation breath frequency is associated with median overnight levels of neural ventilatory drive (calibrated diaphragm EMG in $\%_{eupnea}$; certain + possible: $R^2 = 0.29$, $p < 0.01$) and esophageal pressure swings (cmH_2O; certain

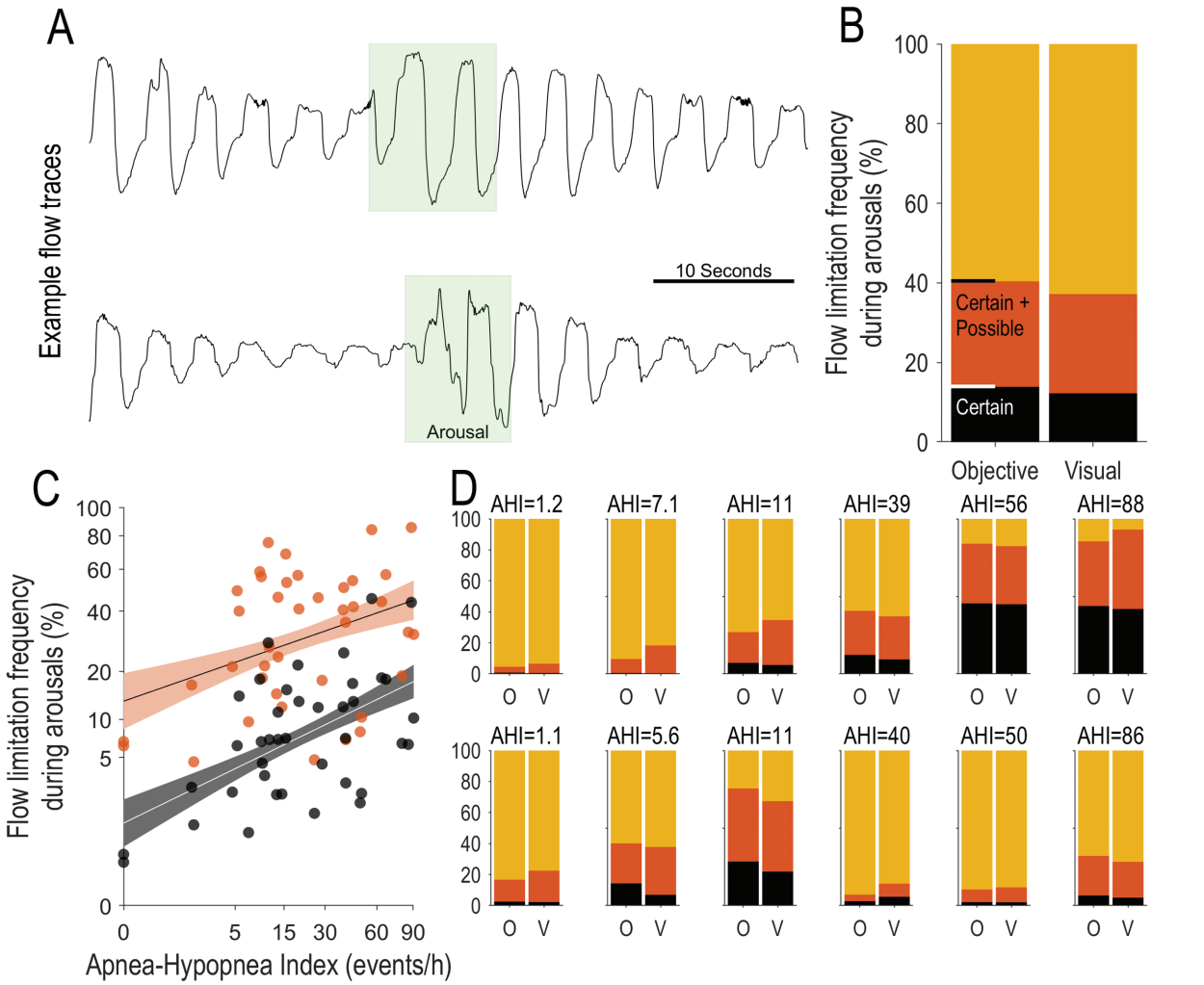

Figure 5. Flow limitation frequency during arousals. (A) Representative airflow recordings from two participants, showing (top) arousal breaths without flow limitation, and (bottom) arousal breaths with flow limitation. (B) Stacked bar chart showing the group mean flow limitation frequency during arousals. (C) Scatter plot showing the relationship between flow limitation frequency during arousals and the apnea-hypopnea index (AHI; orange dots show certain + possible flow limitation, $R^2 = 0.14$, $p < 0.05$; black dots show certain flow limitation, $R^2 = 0.3$, $p < 0.001$). (D) Stacked bar charts for example individual participants; note that some individuals with similar AHI exhibit remarkably different levels of flow limitation during arousals. Certain flow limitation = black, possible flow limitation = orange, and normal = yellow. Objective flow-shape model scoring (O) and visual scoring (V).

+ possible: $R^2 = 0.26$, $p < 0.01$). In contrast, we observed no relationship between AHI and drive ($R^2 < 0.01$, $p = 0.7$) or esophageal pressures ($R^2 < 0.01$, $p = 0.9$). See Supplement Figures S7 and S8.

Discussion

The current study presents a unique library containing physiologically informed visually scored polysomnographic data describing the certainty of pharyngeal airflow obstruction ("flow limitation") on a breath-by-breath basis. Our approach overcame inherent limitations of classification based on visual inspection alone [14, 16, 19, 22, 23, 30, 31] or from physiological signals without the benefit of visual oversight [2, 16, 20, 32, 33]. We then leveraged this library to develop a translatable means to automatically and objectively label individual breaths with a quantitative likelihood of flow limitation (agreement $\kappa = 0.57$, 2-class accuracy = 94%). The use of the method to quantify the prevalence of flow limitation within participants (flow limitation breath frequency) demonstrated minimal error as compared to physiologically informed visual classification ($R^2 = 0.86$, error = 7.2%, certain + possible). The same model remained similarly effective using the clinical airflow surrogate (linearized nasal pressure, also $R^2 = 0.86$, error = 13.4%, certain + possible), confirming clinical applicability. Across patients, flow limitation frequency was only modestly associated with sleep apnea disease severity ($R^2 = 0.16$ *v.* AHI), highlighting that the measure provides distinct information that is otherwise unavailable. The use of a means to objectively quantify flow limitation may facilitate more advanced diagnostic phenotyping and ready identification of patients with symptomatic sleep-disordered breathing that is not manifest as periodic apneas/hypopneas.

Flow limitation resource library

Visually scored physiologically informed airflow obstruction. Our visual scoring protocol incorporates physiological data and therefore provides a unique "library" for the development of model-based flow limitation detection. There are several key

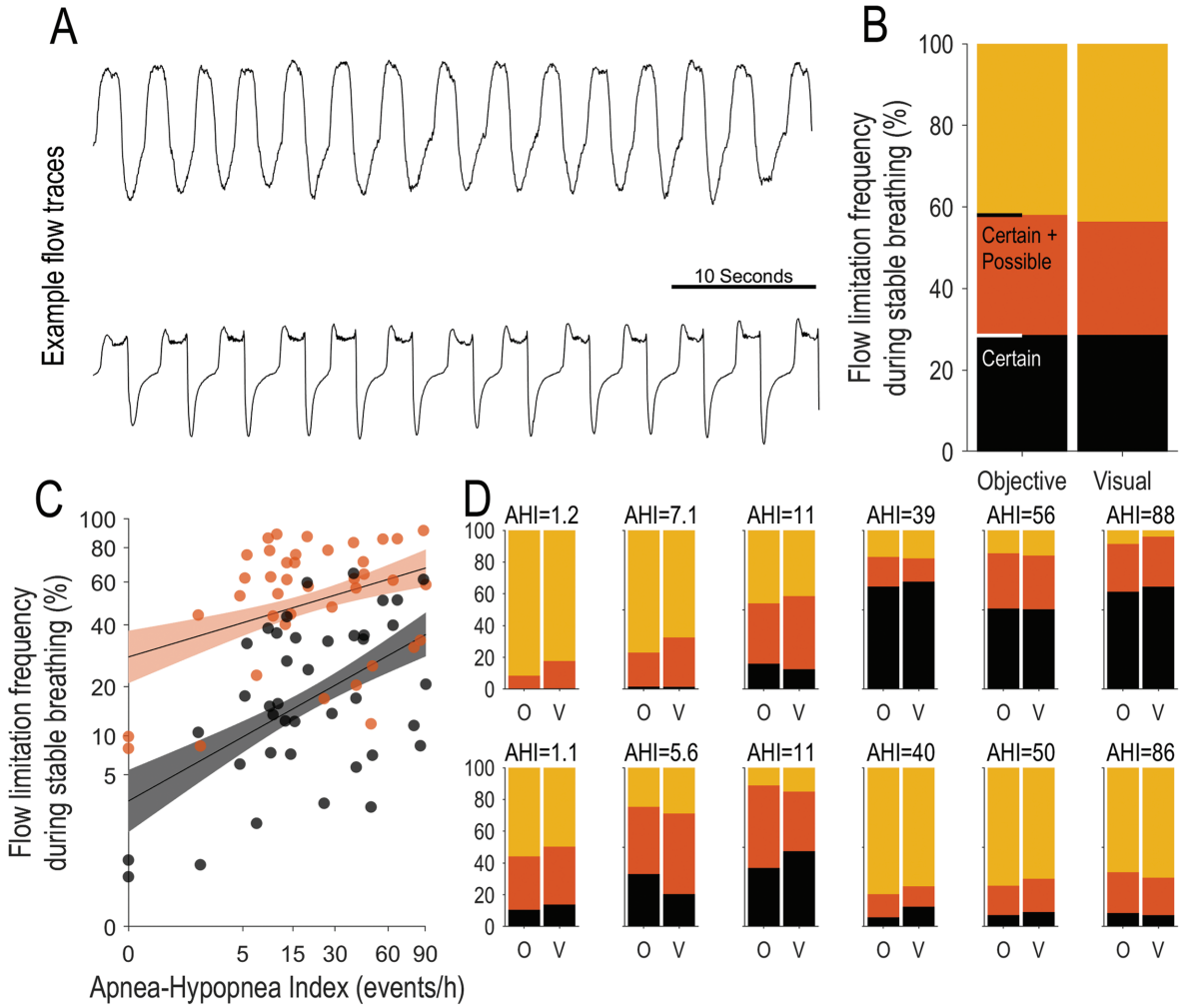

Figure 6. Flow limitation frequency during "stable breathing" (continuous period of >3 min of uninterrupted breathing during sleep, without arousal or scored respiratory event). (A) Representative airflow recordings from two participants, showing (top) stable breathing period without flow limitation, and (bottom) stable breathing period with flow limitation. (B) Stacked bar chart showing the group mean flow limitation frequency during periods of stable breathing. (C) Scatter plot showing the relationship between flow limitation frequency during stable breathing and the apnea-hypopnea index (AHI; orange dots show certain + possible flow limitation, $R^2 = 0.12$, $p < 0.05$; black dots show certain flow limitation, $R^2 = 0.26$, $p < 0.001$). (D) Stacked bar charts for example individual participants; note that some individuals with similar AHI exhibit remarkably different levels of flow limitation during stable breathing. Certain flow limitation = black, possible flow limitation = orange, and normal = yellow. Objective flow-shape model scoring (O) and visual scoring (V).

differences between our visual scoring and previous visual scoring methods [14, 16, 22, 23, 30, 31, 34]. No previous visual scoring methods have utilized gold standard flow-limitation signals to indicate how close flow is to intended flow (i.e. drive) to aide classification. Some studies used measures of epiglottic/esophageal pressures to support visual scoring [22, 23] some fully published classification models that others can apply to airflow signals [22]; others used multiple features acknowledging the heterogeneity in the manifestation of flow limitation across subjects [14, 15, 23, 35]; however, no study met each of these criteria to present a robust translatable model. Our method was strengthened by adopting the following: (1) the entire flow shape, including both inspiratory and expiratory components are incorporated in our method; (2) our protocol includes an intermediate category (possible flow limitation) to acknowledge the inherent nature of uncertainty in interpreting a continuum of obstruction and borderline cases; and (3) scorers gained unique expertise in recognizing how airflow shape reveals airflow obstruction through comprehensive early review of physiological signals and advanced training under experienced physiologists. The analysis also confirmed robustness and validity. Scorers demonstrated excellent interscorer agreement ($\kappa = 0.74$), exceeding all model performance measures. We also found that associations between visual scoring and airflow shapes were stronger than those between physiological signals (*flow:drive* ratio) and airflow shapes, illustrating that visual scoring improved upon the available physiological information.

Library of flow-limited breaths as a resource. Currently, there is no consensus among experts as to what level of flow shape derangement should be classified as flow limitation clinically [1]. Thus, a major additional objective of our study was to provide a library of breaths with various levels of flow limitation as a means to calibrate interpretation of flow limitation across clinical and academic centers internationally. Figure 2 shows a series of breaths—for a single participant—classified as normal, possible flow limitation, and certain flow limitation, with their accompanying objective probabilities of flow

limitation (model output). A comprehensive library of traces is provided in the Supplement (pneumotach in Appendix A, nasal pressure *v.* pneumotach in Appendix B). For each participant, the library illustrates the spectrum of increasing certainty of airflow obstruction, with the corresponding derangement of airflow shape. These data reveal that the nature of obstruction appears heterogeneous across patients (hence requirement for multiple features in final models beyond flattening and scooping [2]) and that breaths often appear near-rounded upon initial inspection but upon detailed review reveal patterns indicating obstruction. A careful review of this library may be useful in training clinicians, investigators, and technicians to recognize the range of flow characteristics associated with flow limitation and the degree of abnormality considered normal *v.* flow-limited. Finally, current advances in machine learning suggest that this library may also prove useful in training new models that aim to reduce subjectivity while continuing to provide insight into clinical flow limitation and its sequalae.

Novel insights

What threshold levels of obstruction appear flow limited? Prior to the current study, we lacked a means to use airflow shapes to objectively classify whether a breath was obstructed (flow limited). Notably, prior work provided a method to estimate the severity of airflow obstruction (*flow:drive*, a continuous variable capturing neuromechanical conductance) continuously using airflow shape; however, this method did not use input from human visual scoring (which we now know strengthens the model). It was also unclear how to use the measure to assess flow limitation frequency (a desired clinical parameter [25, 36, 37]), as the threshold physiological deficit (airflow obstruction) that is manifest clinically (per visual analysis of airflow shapes) was undefined. As part of the current study, we found that: airflow obstruction is typically classified as *possibly* flow limited when *flow:drive* ratio falls below 86%, that is, when drive rises by one-sixth without an increased airflow. While this derangement may sound minimal we note that (1) this threshold is similar to a 2 cmH_2O increase in esophageal pressure swings from a 10 cmH_2O baseline, double the 1 cmH_2O threshold used previously [32, 38, 39], (2) visual inspection of traces in this class reveals clear flow abnormalities. Airflow obstruction is scored as *certainly* flow limited (*v.* possible or normal) when *flow:drive* ratio falls below a 58% threshold. Thus, periods of certain flow limitation may be interpreted to exhibit at least doubled respiratory drive/effort levels (note drive rises with obstruction more than flow falls, due to chemoreflex compensation [3, 40]). For binary classification, airflow obstruction is scored as flow limited (certain *v.* normal) when airflow was at or below 70% of the intended level, consistent with clinical scoring of hypopneas (30% reduction in airflow [41]).

Unique information beyond AHI. Our objective patient-level measures of flow limitation frequency provide information that is not routinely available. First, we emphasize that flow limitation frequency was only modestly associated with disease severity as measured by the AHI (Figure 6) in our study of patients with suspected or diagnosed OSA. Notably, the vast majority of participants referred for evaluation of OSA but without moderate-severe OSA in our study (*N* = 16/18) exhibited flow limitation (certain + possible) for a clinically meaningful duration (>30% of total sleep time; per prior definition of *upper airway resistance syndrome* [24, 25]): a third of these participants exhibited certain flow limitation (*N* = 6/18) for over 30% of total sleep time. On the other hand, about a third (*N* = 8/22) of OSA patients did *not* have certain flow limitation for over 30% of total sleep time. Thus, higher AHI does not necessarily indicate increased flow limitation frequency (or greater risk of any flow-limitation specific sequelae). Second, in additional analysis, we demonstrated that greater flow limitation frequency is associated with (median) overnight levels of neural drive and intrathoracic pressure swings (Supplemental Figures S7 and S8); by contrast, we observed no relationship between AHI and drive or intrathoracic pressures, confirming the notion that measurement of flow limitation may capture unique clinically relevant information.

Insight into flow limitation during arousals and stable breathing. Application of our method demonstrated that—in patients with OSA—flow limitation (certain or possible) is surprisingly prevalent (81[36–100]% of breaths, mean[range]), and is also common during arousals (40[5–85]%) and stable breathing (58[12–91]%), with a wide variety across patients. These data demonstrate that some (but not all) participants exhibit substantial flow limitation during their arousal-related recovery periods; notably, failure to fully recover between events is associated with adverse outcomes [42] and maybe a distinct phenotype. Some participants exhibit substantial flow limitation during stable breathing periods, that is, when breathing is conventionally assumed to no longer require medical intervention, while others appear to achieve stable breathing with minimal flow limitation. It is now possible to examine the implications for sleep apnea sequalae through further investigation.

Clinical implications

Currently, there is a major clinical need for a noninvasive automated method to quantify the frequency of flow-limitation (airflow obstruction) for the purposes of detecting obstructive sleep-disordered breathing in patients without overt OSA, as well as for providing insight into OSA phenotypes (e.g. higher vs. lower ventilatory drive/effort). It is understood that both the symptoms and sequalae of sleep-disordered breathing are not fully captured by the frequency of respiratory events (AHI) [43–45]. In particular, there are numerous symptomatic individuals who exhibit unrecognized flow limitation for a substantial proportion of the night [8, 46–48] who may benefit from treatment [5–11]. The corollary is that many patients currently diagnosed (using AHI) may not have a phenotype of sleep-disordered breathing that has a major impact on daytime function or outcomes. A large body of accumulated evidence now points to an independent role for flow limitation in the adverse outcomes of pharyngeal obstruction, independent of event frequency. Measures of flow limitation have been associated with hypertension and sleepiness independent of the AHI [5–11, 37, 49]. Surgical treatment to address flow limitation in children and adults has been effective at relieving symptoms [8, 9]. CPAP treatment of flow limitation in pregnancy can improve preeclampsia [10].

The current study provides a validated, automated, open-source method to classify flow limitation objectively from polysomnographic airflow, overcoming the prior lack of suitable techniques [1], to potentially enable flow limitation to be routinely assessed clinically. Our method requires no visual scoring, does not require especially high sampling rates by design (25 Hz per AASM minimum requirement [41]), and applies with equivalent validity (similar error) in pneumotach flow and unfiltered nasal pressure. We caution that high pass filtering should not be applied to airflow signals due to baseline distortion that inherently conflates inspiration and expiration and warps the observed airflow shapes required for analysis.

Our work will facilitate trials of interventions in symptomatic patients without markedly elevated AHI levels, or patient groups where negative intrathoracic pressure swings may be pertinent (children, women, pregnancy, comorbid asthma [50], or heart failure [51, 52]), since an objective measure of flow limitation frequency is needed to provide study endpoints. Our work also provides a means to analyze cohort studies investigating links between flow limitation and outcomes in adults.

A further major goal of our work is to provide a means to classify events with versus without flow limitation, which has implications for the classification of obstructive/central hypopneas (central hypopneas are notably defined by the absence of flow limitation). The clinical impact of other novel phenotypes, such as "high AHI with minimal flow limitation" (may respond poorly to existing anatomical interventions) [53–55] or "frequent flow limitation during arousals" (may be at heightened risk of adverse outcomes) [42] is also promising and warrants further investigation. Clinical measurement of flow limitation may also have application in the discrimination between obstructive and central hypoventilation disorders.

Limitations

We considered several limitations. (1) Airflow shape analysis inherently requires reasonable quality of (nasal pressure) airflow signals; thus, our algorithm (and others) will not apply to excessively smoothed, excessively distorted (baseline-drift "corrected"), clipped, or noisy data. However, effort was made to ensure our work was generalizable by using airflow signals downsampled to 25 Hz. (2) While our model was developed using pneumotachograph airflow signals data, we emphasize that we used features that are not affected by the method of measuring airflow (pneumotach *v.* nasal pressure), and the measures performed well in secondary testing using concurrent measures of nasal pressure. (3) Although we sought to avoid the need to calibrate our method on an individual basis, it is possible that individual calibration could optimize flow limitation detection. To examine this possibility, we used each participant's wakefulness flow limitation scores (median probability) to adjust all their overnight results (linear shift of logit[probability] such that the median wake value was equal to the study average of 0.25). Notably, there was no improvement in agreement (κ = 0.552 *v.* 0.572 without the procedure), see Supplement—Assessment of individualized calibration. (4) We intentionally used airflow shape analysis alone for the maximal translatability of our work. While other information is also likely to improve flow limitation prediction (snoring sounds, inductance plethysmography paradox), these signals are subject to marked cross-platform heterogeneity (microphone vs. accelerometer, sensor position; true inductance vs. piezo-electric, filtering settings) that must be handled before multi-signal methods can be used across platforms. (5) The definition of flow limitation used in the current study is intentionally broad to encapsulate the remarkable heterogeneity of ways in which pharyngeal airflow obstruction is visible as a non-rounded airflow shape (including flattening, scooping, jaggedness, fluttering, see the library in Supplement); thus the application of our method to detect a narrower definition based on flatness alone would not be appropriate. (6) Due to resource constraints, our second independent scorer assessed a subset of breaths from each of the participants' data. The subset (a concatenation of breaths from three separate time periods per study) was carefully considered and aimed to capture a broad range of breaths and variability that may exist across the study duration.

Conclusion

The current study developed a library of physiologically informed, visually interpreted airflow shape data from which we present an automated objective means to calculate certainty and frequency of flow-limitation during sleep. Our approach enables quantification of an aspect of sleep-disordered breathing that is otherwise neglected in the clinical evaluation of sleep-disordered breathing where esophageal catheterization is unfeasible. We showed that flow limitation frequency is only modestly associated with AHI, captures the elevated neural drive and ventilatory effort, and is surprisingly frequent during periods of stable breathing and arousals in many patients.

Supplementary Material

Supplementary material is available at *SLEEP* online.

Funding

This work was supported by grants from the National Health and Medical Research Council of Australia (NHMRC 1064163; Dr. Terrill) and the American Heart Association (15SDG25890059; Dr. Sands). Dr. Mann was supported by a University of Queensland Research Scholarship and Graduate School International Travel Award. Dr. Edwards was supported by a Heart Foundation of Australia Future Leader Fellowship (101167). Dr. Azarbarzin was supported by the National Institutes of Health (R01HL153874), American Heart Association (19CDA34660137), and the American Academy of Sleep Medicine Foundation (188-SR-17). Dr. Vena was supported by the American Heart Association (20POST35210530). Dr. Wellman was funded by grants from the NIH (R01 HL102321, R01 HL128658, and P01 HL149630). Drs. Redline, Azarbarzin, and Sands were partially supported by NIH grant R35HL135818. Dr. Sands was supported by the National Institute of Health (NIH; R01HL146697) and an AASM Foundation Strategic Research Award (228-SR-20).

Acknowledgment

The authors are grateful to Maquet Getinge Group for the loan of the intra-esophageal diaphragm EMG recording system.

Disclosure Statement

Financial Disclosure

This was not an industry-sponsored study. Dr Edwards has received grants from Apnimed and has served as a consultant for Signifier Medical. Dr. Azarbarzin serves as a consultant for Somnifix, Inspire, and Apnimed and receives grant money from Somnifix. Dr Wellman works as a consultant for Apnimed, Nox, Inspire, and Somnifix. He has received grants from Sanofi and Somnifix. He also has a financial interest in Apnimed Corp., a company developing pharmacologic therapies for sleep apnea. Dr. Wellman holds a patent on flow shape analysis to detect the site of airway collapse. Dr. Wellman's interests were reviewed and are managed by Brigham and Women's Hospital and Partners HealthCare in accordance with their conflict of interest policies. Dr. Redline received grant funds from Jazz Pharma and consulting fees from Apnimed, RespirCardia, Jazz Inc, and Eisai, unrelated to this article. Dr. Sands receives grant money from Apnimed, Prosomnus, Dynaflex, and has served as a consultant for Apnimed, Nox Medical, and Merck.

Nonfinancial Disclosure

None.

Authors' contributions: Study design: DM, TG, SS, PT; Algorithm development: DM, AA, DV, SS; Sleep and arousal scoring: LH; Visual scoring of flow limitation: TG, SL; Interpretation of results and preparation of the manuscript: All authors.

Data availability statement: Data will be shared on request to the corresponding author with the permission of Brigham and Women's Hospital.

References

1. Pamidi S, *et al.*; American Thoracic Society Ad Hoc Committee on Inspiratory Flow Limitation. An Official American Thoracic Society Workshop Report: noninvasive identification of inspiratory flow limitation in sleep studies. *Ann Am Thorac Soc*. 2017;**14**(7):1076–1085.
2. Mann DL, *et al*. Quantifying the magnitude of pharyngeal obstruction during sleep using airflow shape. *Eur Respir J*. 2019;**54**(1):1802262.
3. de Melo CM, *et al*. Stable breathing in patients with obstructive sleep apnea is associated with increased effort but not lowered metabolic rate. *Sleep*. 2017;**40**(10). doi:10.1093/sleep/zsx128.
4. Calero G, *et al*. Physiological consequences of prolonged periods of flow limitation in patients with sleep apnea hypopnea syndrome. *Respir Med*. 2006;**100**(5):813–817.
5. Nakano H, *et al*. Mean tracheal sound energy during sleep is related to daytime blood pressure. *Sleep*. 2013;**36**(9):1361–1367. doi:10.5665/sleep.2966.
6. Stoohs R, *et al*. Snoring during NREM sleep: respiratory timing, esophageal pressure and EEG arousal. *Respir Physiol*. 1991;**85**(2):151–167.
7. Guilleminault C, *et al*. Upper airway resistance syndrome, nocturnal blood pressure monitoring, and borderline hypertension. *Chest*. 1996;**109**(4):901–908.
8. Guilleminault C, *et al*. Children and nocturnal snoring: evaluation of the effects of sleep related respiratory resistive load and daytime functioning. *Eur J Pediatr*. 1982;**139**(3):165–171.
9. Newman JP, *et al*. Recognition and surgical management of the upper airway resistance syndrome. *Laryngoscope*. 1996;**106**(9 Pt 1):1089–1093.
10. Edwards N, *et al*. Nasal continuous positive airway pressure reduces sleep-induced blood pressure increments in preeclampsia. *Am J Respir Crit Care Med*. 2000;**162**(1):252–257.
11. Pépin JL, *et al*. The upper airway resistance syndrome. *Respiration*. 2012;**83**(6):559–566.
12. Guilleminault C, *et al*. Arousal, increased respiratory efforts, blood pressure and obstructive sleep apnoea. *J Sleep Res*. 1995;**4**(S1):117–124.
13. Chandra S, *et al*. Respiratory effort-related arousals contribute to sympathetic modulation of heart rate variability. *Sleep Breath*. 2013;**17**(4):1193–1200.
14. Zhi YX, *et al*. Detecting inspiratory flow limitation with temporal features of nasal airflow. *Sleep Med*. 2018;**48**:70–78.
15. Aittokallio T, *et al*. Inspiratory flow shape clustering: an automated method to monitor upper airway performance during sleep. *Comput Methods Programs Biomed*. 2007;**85**(1):8–18.
16. Clark SA, *et al*. Assessment of inspiratory flow limitation invasively and noninvasively during sleep. *Am J Respir Crit Care Med*. 1998;**158**(3):713–722.
17. Mooney AM, *et al*. Relative prolongation of inspiratory time predicts high versus low resistance categorization of hypopneas. *J Clin Sleep Med*. 2012;**8**(2):177–185.
18. Teschler H, *et al*. Automated continuous positive airway pressure titration for obstructive sleep apnea syndrome. *Am J Respir Crit Care Med*. 1996;**154**(3 Pt 1):734–740.
19. Camassa A, *et al*. Validating an algorithm for automatic scoring of Inspiratory Flow Limitation within a range of recording settings. In: Proceedings from the 40th Annual International Conference of the IEEE Engineering in Medicine & Biology Society (EMBC); 2018; Honolulu, HI, USA.
20. Morgenstern C, *et al*. Characterization of inspiratory flow limitation during sleep with an exponential model. *Annu Int Conf IEEE Eng Med Biol Soc*. 2008;**2008**:2439–2442.
21. Morgenstern C, *et al*. Automatic differentiation of obstructive and central hypopneas with esophageal pressure measurement during sleep. *Annu Int Conf IEEE Eng Med Biol Soc*. 2009;**2009**:7102–7105.
22. Mansour KF, *et al*. Noninvasive determination of upper airway resistance and flow limitation. *J Appl Physiol*. 2004;**97**(5):1840–1848.
23. Kaplan V, *et al*. Detection of inspiratory flow limitation during sleep by computer assisted respiratory inductive plethysmography. *Eur Respir J*. 2000;**15**(3):570–578.
24. Arora N, *et al*. The role of flow limitation as an important diagnostic tool and clinical finding in mild sleep-disordered breathing. *Sleep Sci*. 2015;**8**(3):134–142.
25. Palombini LO, *et al*. Inspiratory flow limitation in a normal population of adults in São Paulo, Brazil. *Sleep*. 2013;**36**(11):1663–1668. doi:10.5665/sleep.3122.
26. Guyon I, *et al*. An introduction to variable and feature selection. *J Mach Learn Res*. 2003;**3**:1157–1182.
27. Somol P, *et al*. Adaptive floating search methods in feature selection. *Pattern Recogn Lett*. 1999;**20**(11):1157–1163.
28. Youden WJ. Index for rating diagnostic tests. *Cancer*. 1950;**3**(1):32–35.
29. Jordan AS, *et al*. Airway dilator muscle activity and lung volume during stable breathing in obstructive sleep apnea. *Sleep*. 2009;**32**(3):361–368. doi:10.1093/sleep/32.3.361.
30. Miller MR, *et al*. The rise and dwell time for peak expiratory flow in patients with and without airflow limitation. *Am J Respir Crit Care Med*. 1998;**158**(1):23–27.
31. Onal E, *et al*. Respiratory timing during NREM sleep in patients with occlusive sleep apnea. *J Appl Physiol (1985)*. 1986;**61**(4):1444–1448.

32. Mansour KF, *et al*. A mathematical model to detect inspiratory flow limitation during sleep. *J Appl Physiol*. 2002;**93**(3):1084–1092.
33. Morgenstern C, *et al*. Comparison of upper airway respiratory resistance measurements with the esophageal pressure/airflow relationship during sleep. *Annu Int Conf IEEE Eng Med Biol Soc*. 2011;**2011**:3205–3208.
34. Hosselet JJ, *et al*. Detection of flow limitation with a nasal cannula/pressure transducer system. *Am J Respir Crit Care Med*. 1998;**157**(5 Pt 1):1461–1467.
35. Morgenstern C, *et al*. Automatic non-invasive differentiation of obstructive and central hypopneas with nasal airflow compared to esophageal pressure. *Annu Int Conf IEEE Eng Med Biol Soc*. 2010;**2010**:6142–6145.
36. Connolly G, *et al*. Inspiratory flow limitation during sleep in pre-eclampsia: comparison with normal pregnant and nonpregnant women. *Eur Respir J*. 2001;**18**(4):672–676.
37. de Godoy LB, *et al*. Upper airway resistance syndrome patients have worse sleep quality compared to mild obstructive sleep apnea. *PLoS One*. 2016;**11**(5):e0156244.
38. Maddison KJ, *et al*. Effects on upper airway collapsibility of presence of a pharyngeal catheter. *J Sleep Res*. 2015;**24**(1):92–99.
39. Patil SP, *et al*. Neuromechanical control of upper airway patency during sleep. *J Appl Physiol*. 2007;**102**(2):547–556.
40. Eckert DJ, *et al*. Defining phenotypic causes of obstructive sleep apnea. Identification of novel therapeutic targets. *Am J Respir Crit Care Med*. 2013;**188**(8):996–1004.
41. Iber C, *et al*. *The AASM Manual for the Scoring of Sleep and Associated Events: Rules, Terminology and Technical Specifications*. 1st ed. Westchester, IL: American Academy of Sleep Medicine; 2007.
42. Pham LV, *et al*. Oxyhemoglobin saturation overshoot following obstructive breathing events mitigates sleep apnea-induced glucose elevations. *Front Endocrinol*. 2018;**9**:477.
43. Arnardottir ES, *et al*. Obstructive sleep apnoea in the general population: highly prevalent but minimal symptoms. *Eur Respir J*. 2016;**47**(1):194–202.
44. Won CHJ, *et al*. Varying hypopnea definitions affect obstructive sleep apnea severity classification and association with cardiovascular disease. *J Clin Sleep Med*. 2018;**14**(12):1987–1994.
45. Chowdhuri S, *et al*.; ATS Ad Hoc Committee on Mild Obstructive Sleep Apnea. An Official American Thoracic Society Research Statement: impact of mild obstructive sleep apnea in adults. *Am J Respir Crit Care Med*. 2016;**193**(9):e37–e54.
46. Downey R 3rd, *et al*. Upper airway resistance syndrome: sick, symptomatic but underrecognized. *Sleep*. 1993;**16**(7):620–623. doi:10.1093/sleep/16.7.620.
47. Douglas NJ. Upper airway resistance syndrome is not a distinct syndrome. *Am J Respir Crit Care Med*. 2000;**161**(5):1413–1415.
48. Rees K, *et al*. Frequency and significance of increased upper airway resistance during sleep. *Am J Respir Crit Care Med*. 2000;**162**(4 Pt 1):1210–1214.
49. So SJ, *et al*. A comparison of personality characteristics and psychiatric symptomatology between upper airway resistance syndrome and obstructive sleep apnea syndrome. *Psychiatry Investig*. 2015;**12**(2):183–189.
50. Cao X, *et al*. Effect of simulated obstructive sleep apnea on thoracic fluid volume and lower airway resistance in asthmatics. *Eur Respir J*. 2020;**56**.
51. Bradley TD, *et al*. Cardiac output response to continuous positive airway pressure in congestive heart failure. *Am Rev Respir Dis*. 1992;**145**(2 Pt 1):377–382.
52. Kaneko Y, *et al*. Cardiovascular effects of continuous positive airway pressure in patients with heart failure and obstructive sleep apnea. *N Engl J Med*. 2003;**348**(13):1233–1241.
53. Bradley TD, *et al*.; CANPAP Investigators. Continuous positive airway pressure for central sleep apnea and heart failure. *N Engl J Med*. 2005;**353**(19):2025–2033.
54. Edwards BA, *et al*. Upper-airway collapsibility and loop gain predict the response to oral appliance therapy in patients with obstructive sleep apnea. *Am J Respir Crit Care Med*. 2016;**194**(11):1413–1422.
55. Joosten SA, *et al*. Loop gain predicts the response to upper airway surgery in patients with obstructive sleep apnea. *Sleep*. 2017;**40**(7). doi:10.1093/sleep/zsx094.